arXiv:1703.07300v1 [math.NA] 21 Mar 2017

IMA Journal of Numerical Analysis (2017) Page 1 of 19
doi:10.1093/imanum/drn000

A stroboscopic averaging algorithm for highly oscillatory delay problems

J. M. SANZ-SERNA†
Departamento de Matemáticas, Universidad Carlos III de Madrid,
Avenida de la Universidad 30, E-28911 Leganés (Madrid), Spain

AND

BEIBEI ZHU‡

LSEC, ICMSEC, Academy of Mathematics and Systems Science,
Chinese Academy of Sciences, Beijing 100190, China

[Received on 22 March 2017]

We propose and analyze a heterogenous multiscale method for the efficient integration of constant-delay differential equations subject to fast periodic forcing. The stroboscopic averaging method (SAM) suggested here may provide approximations with $\mathscr{O}(H^2+1/\Omega^2)$ errors with a computational effort that grows like H^{-1} (the inverse of the stepsize), uniformly in the forcing frequency Ω.

Keywords: Delay differential equations, stroboscopic averaging, highly oscillatory problems

1. Introduction

We propose and analyze a heterogenous multiscale method (HMM) (E, 2003; E & Engquist, 2003) for the efficient integration of constant-delay differential equations subject to fast periodic forcing. The stroboscopic averaging method (SAM) suggested here may provide approximations with $\mathscr{O}(H^2+1/\Omega^2)$ errors with a computational effort that grows like H^{-1} (the inverse of the stepsize), uniformly in the forcing frequency Ω.

The numerical integration of highly oscillatory differential equations or delay differential equations may be a very demanding task, as standard methods typically have to employ timesteps smaller than the periods present in the solution. For systems without delay, the literature contains many suggestions of numerical schemes specially designed to operate in the highly-oscillatory scenario; many of them are reviewed in Hairer et al. (2002). Perhaps counterintuitively, some of those methodologies take advantage of the large frequency and their efficiency actually increases with Ω (Iserles & Nørsett, 2005). On the other hand, schemes for highly oscillatory problems may suffer from unexpected instabilities and inaccuracies (Calvo & Sanz-Serna, 2009).

The algorithm suggested here is based on ideas presented, for systems without delay, in Calvo et al. (2011a) and Calvo et al. (2011b). In these references, given an oscillatory problem, a *stroboscopically averaged* problem is introduced such that, at the stroboscopic times $t^{(k)}=kT$, $T=2\pi/\Omega$, $h=0,1,\ldots$, its solution $X(t)$ (approximately) coincides with the true oscillatory solution x.[1] The stroboscopically

†Email: jmsanzserna@gmail.com
‡Corresponding author. Email: zhubeibei@lsec.cc.ac.cn

[1]The notion of stroboscopic averaging studied in detail in Chartier et al. (2012) is far from new. However standard treatments of the theory of averaging favour alternative techniques, specially the zero-mean approach where the functions necessary to express

© The author 2017. Published by Oxford University Press on behalf of the Institute of Mathematics and its Applications. All rights reserved.

averaged problem does not include rapidly varying forcing terms and therefore, if available in closed form, may be integrated numerically without much ado. The algorithms in Calvo et al. (2011a) and Calvo et al. (2011b) compute numerically values of X, without demanding that the user finds analytically the expression of the averaged system. More precisely, the algorithms only require evaluations of the right hand-side of the originally given oscillatory problem. The solution X is advanced with a standard integrator (the macro-integrator) with a stepsize H that, for a target accuracy, may be chosen to be independent of Ω. When the macro-integrator requires a value F of the slope $\dot{X}$, F is found by numerical differentiation of a micro-solution u, i.e. a solution of the originally given oscillatory problem. While the micro-integrations to find u are performed with stepsizes h that are a submultiple of the (small) period T, the corresponding computational cost does not increase as $\Omega \to \infty$, because u is only required in windows of width mT, m a small integer.

Our research was motivated by the study of the phenomenon of vibrational resonance (Landa & McClintock, 2000) in a genetic toggle switch (Gardner et al., 2000). Although this delay system possesses a very simple analytic expression, its direct numerical integration is not feasible for large values of Ω (see Section 7). The SAM algorithm studied here uses the second-order Adams-Bashforth method for the macro-integrations and micro-integrates with Euler's rule.

The extension of the material in Calvo et al. (2011a) and Calvo et al. (2011b) to the present circumstances is far from trivial. A first difficulty stems from the well-known fact that, in the delay scenario, regardless of the smoothness of the equation, solutions may be non-smooth at points t that are integer multiples of the (constant) delay. Therefore, the algorithm presented here has to make special provision for that lack of smoothness. In addition, the analysis of the algorithm (but, as emphasized above, not the algorithm itself) is built on the knowledge of the stroboscopically averaged systems. While the construction of a stroboscopically averaged system with errors $x(t^{(k)}) - X(t^{(k)}) = \mathscr{O}(1/\Omega)$ is not difficult, here we aim at errors $x(t^{(k)}) - X(t^{(k)}) = \mathscr{O}(1/\Omega^2)$ and this requires much additional analysis. The classical reference Lehman & Weibel (1999) only considers zero-mean, $\mathscr{O}(1/\Omega)$ averaging.

In Section 2 we explain the ideas behind SAM and present a detailed description of the algorithm. Section 3 contains the construction of the stroboscopically averaged system with $\mathscr{O}(1/\Omega^2)$ accuracy. Sections 4 and 5 are devoted to the analysis of SAM. In the first of these, we assume that the micro-integrations carried out in the algorithm are performed exactly. Under suitable hypotheses, the errors in SAM are $\mathscr{O}(H^2 + 1/\Omega^2)$. The effect of the errors in the micro-integration is studied in Section 5: it is shown that, with a computational cost that grows like $1/H$, SAM may yield errors of size $\mathscr{O}(H^2 + 1/\Omega^2)$. The H^2 (second order) behaviour of the error may come as a surprise, because micro-integrations are performed by Euler's rule; of key importance here is a superconvergence result (see the bound in (5.2)) for the Euler solution of oscillatory problems when the integration is carried out over a whole number of periods. The last two sections report numerical experiments that, on the one hand, confirm the theoretical expectations and, on the other, show the advantage of SAM when compared with a direct numerical integration of the oscillatory problem.

2. The stroboscopic averaging method (SAM)

This section motivates and describes the SAM algorithm.

the required change of variables are chosen so as to have zero mean over one period of the oscillation. In stroboscopic averaging the available freedom is used to impose that the old and new variables coincide at stroboscopic times. This is advantageous for the numerical methods studied here, which work at stroboscopic times. The zero-mean approach may be better for analytic purposes at it usually leads to simpler high-order averaged systems,

2.1 *Motivation*

We consider highly oscillatory delay differential systems of the form

$$\begin{aligned} \dot{x}(t) &= f(x(t),y(t),t,\Omega t;\Omega), \qquad t \geqslant 0, \\ y(t) &= x(t-\tau), \qquad t \geqslant 0, \end{aligned} \tag{2.1}$$

where the solution x is defined for $t \geqslant -\tau$ and takes values in $\mathbb{R}^D$, the function $f(x,y,t,\theta;\Omega) : \mathbb{R}^D \times \mathbb{R}^D \times \mathbb{R} \times \mathbb{R} \times \mathbb{R} \to \mathbb{R}^D$ depends 2π–periodically on its fourth argument θ, $\tau > 0$ is the (constant) delay, and the frequency Ω is seen as a parameter, $\Omega \gg 1$. Note that f depends explicitly on t through its third and fourth arguments; the fourth is the *rapidly rotating phase* $\theta = \Omega t$ and the third corresponds to a *slow* (i.e. Ω-independent) dependence on t (see the example below). The values of x on the interval $[-\tau, 0]$ are prescribed through an Ω*–independent*[2] function φ:

$$x(t) = \varphi(t), \qquad -\tau \leqslant t \leqslant 0. \tag{2.2}$$

It is well known that, regardless of the smoothness of f and φ, the function $x(t)$ will typically not be differentiable at $t = 0$ and that in (2.1) $\dot{x}(0)$ has to be understood as a right derivative. Furthermore the discontinuity of $\dot{x}(t)$ at $t = 0$ will lead to the discontinuity of $\ddot{x}(t)$ at $t = \tau$, etc.

We assume that, at the *stroboscopic times* $t^{(k)} = kT$, where $T = 2\pi/\Omega$ is the period and $k = 0, 1, \ldots$, the solution $x(t)$ of the oscillatory delay problem (2.1)–(2.2) may be approximated (in a sense to be made precise later) by the solution $X(t)$ of an averaged problem

$$\begin{aligned} \dot{X}(t) &= F, \qquad t \geqslant 0, \\ X(t) &= \varphi(t), \qquad -\tau \leqslant t \leqslant 0,, \end{aligned} \tag{2.3}$$

where the value of the function F may depend on $X(t)$, on the history $X(s)$, $-\tau \leqslant s < t$, on the slow time t and on Ω but is *independent* of the fastly varying phase $\theta = \Omega t$.

As an illustration we consider the system ($\alpha, \beta, \omega, A, B$ are constants)

$$\begin{aligned} \dot{x}_1(t) &= \frac{\alpha}{1+x_2^\beta(t)} - y_1(t) + A\sin(\omega t) + B\sin(\Omega t), \\ \dot{x}_2(t) &= \frac{\alpha}{1+x_1^\beta(t)} - y_2(t), \end{aligned} \tag{2.4}$$

that for $A = 0, B = 0$ describes a time-delayed genetic toggle switch, a synthetic gene-regulatory network (Gardner et al., 2000). Studied by Daza et al. (2013) is the phenomenon of *vibrational resonance* (Landa & McClintock, 2000), i.e. the way in which the presence of the high-frequency forcing $B\sin(\Omega t)$ enhances the response of the system to the low-frequency forcing $A\sin(\omega t)$. Fig. 1 displays, in a short time interval, a solution of the given oscillatory system and the corresponding averaged solution, found by solving the system

$$\begin{aligned} \dot{X}_1(t) &= \frac{\alpha}{1+X_2^\beta(t)} - Y_1(t) - \frac{B}{\Omega} 1_{\{t \geqslant \tau\}}(t) + A\sin(\omega t), \\ \dot{X}_2(t) &= \frac{\alpha}{1+X_1^\beta(t)} - Y_2(t) - \frac{B}{\Omega} \frac{\alpha\beta X_1^{\beta-1}(t)}{(1+X_1^\beta(t))^2}, \end{aligned} \tag{2.5}$$

[2] Assuming that φ does not depend on Ω implies no loss of generality, as the general case may be reduced to the Ω-independent case by introducing a new dependent variable $x(t) - \Phi(t)$, where $\Phi(t)$ coincides with $\varphi(t)$ for $-\tau \leqslant t \leqslant 0$.

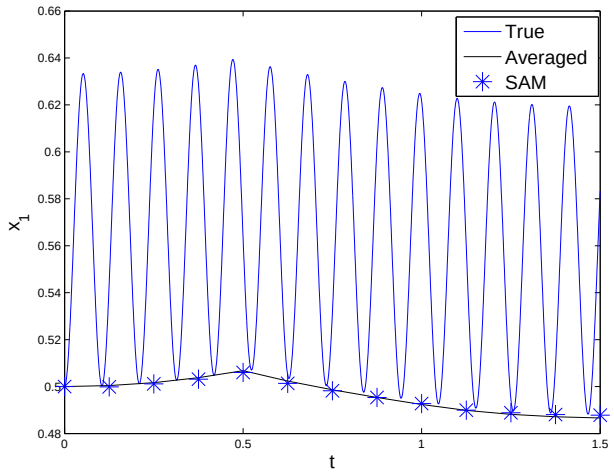

FIG. 1. x_1 component of the toggle switch problem. The constants τ, α, β, A, ω, B, and the function φ are chosen as in Section 6 and $\Omega = 60$. The true solution x and the averaged solution X are very close at the stroboscopic times $t^{(k)} = k(2\pi/\Omega) = kT$, $k = 0, 1, \ldots$ SAM is used to generate approximations to X at the step points $t_n = nH$, $H = 0.125$, $n = 0, 1, \ldots$ In this example the step points are *not* stroboscopic times.

where $Y_i(t) = X_i(t-\tau)$ and $1_{\{t\geqslant\tau\}}(t)$ is the (indicator) function that takes the value 1 for $t \geqslant \tau$ and vanishes for $t < \tau$ (see the next section for the derivation of this averaged system). Note that, due to the presence of $1_{\{t\geqslant\tau\}}(t)$, the right hand-side of the averaged system is discontinuous at $t = \tau$ (this discontinuity manifests itself in Fig. 1 through a discontinuity in the slope of X) and that the slow time-dependent forcing $A\sin(\omega t)$ has not been averaged out. The study of vibrational resonance requires to simulate over long time intervals (the interval $0 \leqslant t \leqslant 300$ is used in Daza et al. (2013)) for many choices of the values of the constants $\alpha, \beta, \omega, A, B, \tau$ and the parameter Ω; the presence of the fast-frequency oscillations makes such a task costly. It is then of interest to simulate, if possible, averaged systems like (2.3) rather than highly-oscillatory models like (2.1). However, obtaining F analytically may be difficult or even impossible and we wish to have a numerical method that approximates X by using only f. SAM is such a technique.

The idea behind SAM is as follows. Let x and X be respectively the oscillatory and averaged solutions corresponding to the same φ. At fixed t, $\dot{x}$ and $\dot{X}$ may differ substantially. However difference quotients such as $(x(t+T)-x(t))/T$ or $(x(t+T)-x(t-T))/(2T)$ may provide a good approximation to the slope $\dot{X}(t)$ (see Fig. 1). As other heterogeneous multiscale methods (see e.g. E (2003); E & Engquist (2003); E et al. (2007); Engquist & Tsai (2005); Li et al. (2007); Ariel et al. (2009); Sanz-Serna (2009); Calvo & Sanz-Serna (2010)), the algorithm includes macro-integrations and micro-integrations. Macro-integations are used to advance X over macro-steps of length H larger than the period T. The necessary slopes $\dot{X}$ are obtained by forming difference quotients of auxiliary oscillatory solutions found by micro-integrations with small steps h.

2.2 *The algorithm*

Let us now describe the algorithm.

2.2.1 *Macro-integration.* Choose a positive integer N and define the macro-stepsize $H = \tau/N$. If the solution is sought in an interval $0 \leqslant t \leqslant t_{max}$, SAM generates approximations X_n to $X(t_n)$, $t_n = nH$,

$n = 0, 1, \ldots, \lfloor t_{max}/H \rfloor$ by using the second-order Adams-Bashforth formula (macro-integrator)

$$X_{n+1} = X_n + \frac{3}{2} H F_n - \frac{1}{2} H F_{n-1}, \tag{2.6}$$

starting from $X_0 = x(0) = X(0) = \varphi(0)$; here F_n is an approximation to $\dot{X}(t_n)$ obtained by numerical differentiation of the micro-solution. The formula is *not* used if $n = 0$ and $n = N$, where it would be inconsistent in view of the jump discontinuities of $\dot{X}$ at $t = 0$ and $t = \tau$ noted above. For $n = 0$ or $n = N$ we use Euler's rule, i.e. we set

$$X_1 = X_0 + H F_0, \qquad X_{N+1} = X_N + H F_N. \tag{2.7}$$

2.2.2 *Micro-integration.* If ν_{max} is a positive integer, the micro-stepsize h is chosen to be T/ν_{max} (recall that $T = 2\pi/\Omega$ denotes the period). We use Euler's rule, starting from $u_{n,0} = X_n$, first to integrate forward the oscillatory problem (2.1) over one period

$$u_{n,\nu+1} = u_{n,\nu} + h f(u_{n,\nu}, v_{n,\nu}, t_n + \nu h, \Omega \nu h; \Omega), \quad \nu = 0, 1, \ldots, \nu_{max} - 1, \tag{2.8}$$

and then to integrate backward over one period

$$u_{n,-\nu-1} = u_{n,-\nu} - h f(u_{n,-\nu}, v_{n,-\nu}, t_n - \nu h, -\Omega \nu h; \Omega), \quad \nu = 0, 1, \ldots, \nu_{max} - 1. \tag{2.9}$$

Here v denotes the past values for u given by $v_{n,\nu} = u_{n-N,\nu}$ if $n > N$, and $v_{n,\nu} = \varphi(-\tau + nH + \nu h)$ for $n < N$ (if $n = N$ $v_{N,\nu} = u_{0,\nu}$ for $\nu \geqslant 0$ and $v_{N,\nu} = \varphi(\nu h)$ for $\nu < 0$).

It is *crucial* to observe the values $\Omega \nu h$ and $-\Omega \nu h$ used for the fast argument θ in (2.8) and (2.9) respectively; each micro-integration starts from $\theta = 0$ rather than from the value $\theta = \Omega t_n$ which may perhaps have been expected. The reason for this is that in stroboscopic averaging, the resulting averaged system changes with the initial value of the phase θ; to work with one and the same averaged system micro-integrations have to start from the value $\theta = 0$ that the phase takes at the initial point of the interval $[0, t_{max}]$ (see Calvo et al. (2011a), Calvo et al. (2011b) for a detailed discussion).

The slopes F_n to be used in (2.6) or (2.7) are given by the central difference formula,

$$F_n = \frac{u_{n,\nu_{max}} - u_{n,-\nu_{max}}}{2T} \tag{2.10}$$

if $n \neq 0$ and $n \neq N$, while for $n = 0$ and $n = N$, we use the forward difference formula

$$F_0 = \frac{u_{0,\nu_{max}} - u_{0,0}}{T}, \qquad F_N = \frac{u_{N,\nu_{max}} - u_{N,0}}{T}, \tag{2.11}$$

due to the discontinuity of $\dot{X}(t)$ at $t = 0$ and $t = \tau$. A detailed description of the algorithm is provided in Table 1.

Fig. 2 may help to better understand the procedure. The upper time axis corresponds to the macro-integration; all the information needed to obtain X_{n+1} is X_n, F_n and F_{n-1} (F_{n-1} is actually not required for $n = 0, N$). The value of F_n is derived by numerical differentiation of the micro-solution and passed to the macro-integrator to compute X_{n+1}. For fixed n, the computation of the Euler micro-solution $u_{n,\nu}$ uses the past values $v_{n,\nu}$ and the initial datum $u_{n,0} = X_n$ (note that X_n is the most recent vector found in the macro-integration).

SAM only operates with macro-stepsizes H that are a submultiple of the delay τ; this restriction is imposed to enforce that $t = \tau$ be a step-point to better deal with the discontinuity in slope at $t = \tau$ (see

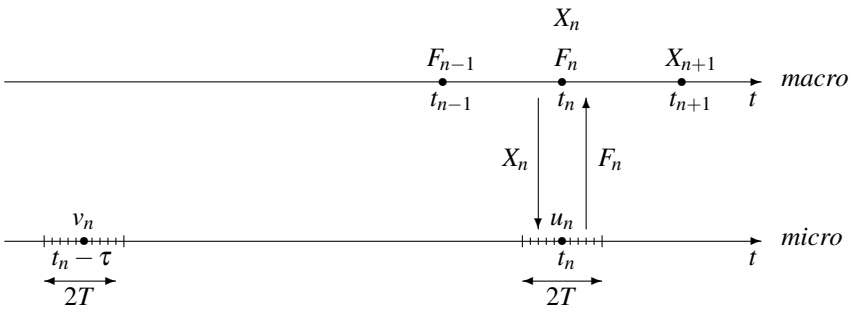

FIG. 2. Schematic description of SAM. Once X_n is available, it is passed to the micro-integrator to find $u_{n,v}$ for varying v. Numerical differentiation of the micro-solution yields F_n which is used in the macro-stepping to compute X_{n+1}

Fig. 1). In general the quotient τ/T will be irrational and then the step points t_n will not be stroboscopic times; this is the case in the simulation in Fig. 1.

We emphasize that, given N and v_{max}, the *complexity* of the algorithm is *independent* of Ω. When Ω increases, the micro-stepsize h decreases to cater for the more rapid variation of the oscillations but the window of width $2T$ (or T) for each micro-integration becomes correspondingly narrower.

Finally we point out that we have tested several alternative algorithms. For instance we alternatively performed the micro-integrations with the Adams-Barshforth second order method, or we used second-order forward approximations for F_0, F_N. While those modifications improve the accuracy of the results for small stepsizes, experiments reveal that they are not always beneficial for large stepsizes; therefore we shall not be concerned with them here.

3. The averaged system

In this section and the three that follow, we assume that the system (2.1) is of the particular form

$$\dot{x}(t) = f(x(t), y(t), \Omega t). \tag{3.1}$$

When comparing with the general format in (2.1) we note that now $f(x,y,\theta)$ has three arguments rather than five. The case where f includes a slow explicit dependence on t i.e. $f = f(x,y,t,\theta)$ may be trivially reduced to (3.1) by adding a component x_{D+1} to the state vector $x \in \mathbb{R}^D$ and setting $\dot{x}_{D+1} = 1$. The case where f depends on Ω, i.e. $f = f(x,y,\theta;\Omega)$ is taken up in the final section. We assume that $f(x,y,\theta)$ and the initial function φ in (2.2) are of class C^3, and that the solution x exists in the interval $[0,t_{max}]$ where t_{max} is a constant (i.e. does not change with the parameter Ω).

Using an approach similar to that in Chartier et al. (2010), Chartier et al. (2012), Chartier et al. (2015), we use a Fourier decomposition

$$f(x,y,\theta) = \sum_{k\in\mathbb{Z}} \exp(ik\theta) f_k(x,y);$$

The coefficients $f_k(x,y)$ satisfy $f_k \equiv f_{-k}^*$ because the problem is real.

It is easily seen that, under the preceding hypotheses, x undergoes oscillations of frequency Ω and amplitude $\mathcal{O}(1/\Omega)$ as $\Omega \to \infty$. To reduce the amplitude of the oscillations to $\mathcal{O}(1/\Omega^2)$, we consider the

Table 1. SAM Algorithm

Compute X_1
  Micro-integration
    $u_{0,0} = \varphi(0)$ % initial value
    For $\nu = 0 : \nu_{max}$, $v_{0,\nu} = \varphi(-\tau + \nu h)$, end % history
    For $\nu = 0 : \nu_{max} - 1$, $u_{0,\nu+1} = u_{0,\nu} + hf(u_{0,\nu}, v_{0,\nu}, t_0 + \nu h, \Omega\nu h; \Omega)$, end % Euler
    $F_0 = (u_{0,\nu_{max}} - u_{0,0})/T$ % slope for macro-step
  Macro-integration
    $t_0 = 0$, $X_0 = \varphi(0)$, $t_1 = t_0 + H$, $X_1 = X_0 + HF_0$ % Euler macro at n=0
Compute $X_2, \ldots, X_N$
For $n = 2 : N$
  Micro-integration
    $u_{n,0} = X_n$ % initial value
    For $\nu = -\nu_{max} : \nu_{max}$, $v_{n,\nu} = \varphi(-\tau + nH + \nu h)$, end % history
    For $\nu = 0 : \nu_{max} - 1$, $u_{n,\nu+1} = u_{n,\nu} + hf(u_{n,\nu}, v_{n,\nu}, t_n + \nu h, \Omega\nu h; \Omega)$
    $u_{n,-\nu-1} = u_{n,-\nu} - hf(u_{n,-\nu}, v_{n,-\nu}, t_n - \nu h, -\Omega\nu h; \Omega)$, end % Euler
    $F_n = (u_{n,\nu_{max}} - u_{n,-\nu_{max}})/(2T)$ % slope for macro-step
  Macro-integration
    $t_{n+1} = t_n + H$, $X_{n+1} = X_n + (3H/2)F_n - (H/2)F_{n-1}$ % Adams-Bashforth2 macro
end
Compute X_{N+1}
  Micro-integration
    $u_{N,0} = X_N$ % initial value
    For $\nu = 1 : \nu_{max}$, $u_{0,-\nu} = \varphi(-\nu h)$, end % values taken from history
    For $\nu = -\nu_{max} : \nu_{max}$, $v_{N,\nu} = u_{0,\nu}$, end % save for later history
    For $\nu = 0 : \nu_{max} - 1$, $u_{N,\nu+1} = u_{N,\nu} + hf(u_{N,\nu}, v_{N,\nu}, t_N + \nu h, \Omega\nu h; \Omega)$
    $u_{N,-\nu-1} = u_{N,-\nu} - hf(u_{N,-\nu}, v_{N,-\nu}, t_N - \nu h, -\Omega\nu h; \Omega)$, end % Euler
    $F_N = (u_{N,\nu_{max}} - u_{N,0})/T$ % slope for macro-step
  Macro-integration
    $t_{N+1} = t_N + H$, $X_{N+1} = X_N + HF_N$ % Euler macro at n=N
Compute $X_{N+2}, \ldots$
For $n = N + 1 : \lfloor t_{max}/H \rfloor$
  Micro-integration
    $u_{n,0} = X_n$ % initial value
    For $\nu = -\nu_{max} : \nu_{max}$, $v_{n,\nu} = u_{n-N,\nu}$, end % save for later history
    For $\nu = 0 : \nu_{max} - 1$, $u_{n,\nu+1} = u_{n,\nu} + hf(u_{n,\nu}, v_{n,\nu}, t_n + \nu h, \Omega\nu h; \Omega)$
    $u_{n,-\nu-1} = u_{n,-\nu} - hf(u_{n,-\nu}, v_{n,-\nu}, t_n - \nu h, -\Omega\nu h; \Omega)$, end % Euler
    $F_n = (u_{n,\nu_{max}} - u_{n,-\nu_{max}})/(2T)$ % slope for macro-step
  Macro-integration
    $t_{n+1} = t_n + H$, $X_{n+1} = X_n + (3H/2)F_n - (H/2)F_{n-1}$ % Adams-Bashforth2 macro
end

near identity change of variables

$$\begin{cases} x = X + \sum_{k\neq 0} \dfrac{\exp(ik\Omega t)-1}{ik\Omega} f_k(X,Y), & t \geqslant 0, \\ x = X, & -\tau \leqslant t < 0. \end{cases} \tag{3.2}$$

so that x and X coincide at stroboscopic times. Before we obtain an averaged system with the help of this change of variables, we introduce some notation. For the past value of $y(t)$, we set $z(t) = y(t-\tau)$, $t \geqslant \tau$. The variables X, Y, Z in the averaged system correspond to x, y, z and we define

$$\alpha_k(t) = \frac{\exp(ik\Omega t)-1}{ik\Omega}, \quad k \in \mathbb{Z}.$$

This $\mathscr{O}(1/\Omega)$ function contains an oscillatory component and the non-oscillatory component $-1/(ik\Omega)$.

The proof of the following result is a straightforward but very lengthy exercise on Taylor expansion.

LEMMA 3.1 *The change of variables (3.2) transforms the system (3.1) into*

$$\begin{aligned} \dot{X} &= f_0 - \sum_{k\neq 0} \alpha_k(t) \frac{\partial f_k}{\partial X} f_0 - \sum_{k\neq 0} \alpha_k(t) \frac{\partial f_k}{\partial Y} \dot{\varphi}(t-\tau) \\ &\quad + \sum_{k\neq 0} \alpha_k(t) \frac{\partial f_0}{\partial X} f_k + \sum_{k,\ell\neq 0} \exp(ik\Omega t)\alpha_\ell(t) \frac{\partial f_k}{\partial X} f_\ell + \mathscr{O}(\frac{1}{\Omega^2}), \end{aligned} \tag{3.3}$$

for $0 \leqslant t < \tau$, *and into*

$$\begin{aligned} \dot{X} &= f_0 - \sum_{k\neq 0} \alpha_k(t) \frac{\partial f_k}{\partial X} f_0 - \sum_{k\neq 0} \alpha_k(t) \frac{\partial f_k}{\partial Y} f_{0\tau} + \sum_{k\neq 0} \alpha_k(t) \frac{\partial f_0}{\partial X} f_k + \sum_{k\neq 0} \alpha_k(t-\tau) \frac{\partial f_0}{\partial Y} f_{k\tau} \\ &\quad + \sum_{k,\ell\neq 0} \exp(ik\Omega t)\alpha_\ell(t) \frac{\partial f_k}{\partial X} f_\ell + \sum_{k,\ell\neq 0} \exp(ik\Omega t)\alpha_\ell(t-\tau) \frac{\partial f_k}{\partial Y} f_{\ell\tau} + \mathscr{O}(\frac{1}{\Omega^2}), \end{aligned} \tag{3.4}$$

for $t \geqslant \tau$. *Here and later*

$$f_k = f_k(X,Y), \qquad f_{k\tau} = f_k(Y,Z), \qquad k \in \mathbb{Z}.$$

Note that system in (3.3)–(3.4) is of the (expected) form

$$\dot{X} = f_0 + \mathscr{O}(1/\Omega), \tag{3.5}$$

where f_0 is the average

$$f_0(X,Y) = \frac{1}{T}\int_0^T f(X,Y,\theta)\,d\theta. \tag{3.6}$$

By suppressing the remainder in (3.5), we obtain the averaged system $\dot{X} = f_0(X,Y)$ with $\mathscr{O}(1/\Omega)$ error; this is not sufficiently accurate for our purposes and we take the averaging procedure to higher order. To do so, we average out the oscillatory terms of size $\mathscr{O}(1/\Omega)$ in the sums in (3.3)–(3.4), i.e. we remove them by performing an additional stroboscopic[3] change of variables (differing from the identity

[3]This means that at stroboscopic times the (periodic) change of variables is the identity, i.e. the old and new variables coincide.

in $\mathcal{O}(1/\Omega^2)$ quantities). In order to keep the notation simple, we shall not introduce a new symbol for the dependent variable after this additional change of variables and we use the symbol X already employed for the old variable.

By suppressing, in the way we have described, the $\mathcal{O}(1/\Omega)$ oscillatory terms in (3.3)–(3.4) and ignoring the $\mathcal{O}(1/\Omega^2)$ remainder, we obtain the averaged system given in (3.7)–(3.9) below, where $[\cdot,\cdot]$ is the Lie-Jacobi bracket or commutator defined by

$$[f_i, f_j] = \frac{\partial f_j}{\partial X} f_i - \frac{\partial f_i}{\partial X} f_j, \quad i, j \in \mathbb{Z}.$$

The averaged solution X will obviously approximate x at stroboscopic times with $\mathcal{O}(1/\Omega^2)$ errors (arising from discarding the $\mathcal{O}(1/\Omega^2)$ remainder); this implies that, at least for Ω sufficiently large, X exists in the interval $[0, t_{max}]$. We then have proved the following result.

THEOREM 3.1 *Consider the averaged problem*

$$\begin{aligned} \dot{X}(t) &= F(X(t), Y(t), Z(t), t; \Omega), \qquad t \geqslant 0, \\ Y(t) &= X(t-\tau), \qquad t \geqslant 0, \\ Z(t) &= Y(t-\tau), \qquad t \geqslant \tau, \\ X(t) &= \varphi(t), \qquad -\tau \leqslant t \leqslant 0, \end{aligned} \tag{3.7}$$

with $F(X,Y,Z,t;\Omega) = F^{(1)}(X,Y,t;\Omega)$,

$$F^{(1)}(X,Y,t;\Omega) = f_0 + \sum_{k>0} \frac{i}{k\Omega} \left([f_k - f_{-k}, f_0] + [f_{-k}, f_k] \right) - \sum_{k \neq 0} \frac{i}{k\Omega} \frac{\partial f_k}{\partial Y} \dot{\varphi}(t-\tau), \tag{3.8}$$

for $0 \leqslant t < \tau$ *and* $F(X,Y,Z,t;\Omega) = F^{(2)}(X,Y,Z;\Omega)$,

$$\begin{aligned} F^{(2)}(X,Y,Z;\Omega) &= f_0 + \sum_{k>0} \frac{i}{k\Omega} \left([f_k - f_{-k}, f_0] + [f_{-k}, f_k] \right) - \sum_{k \neq 0} \frac{i}{k\Omega} \frac{\partial f_k}{\partial Y} f_{0\tau} \\ &\quad + \sum_{k \neq 0} \frac{i}{k\Omega} \frac{\partial f_0}{\partial Y} f_{k\tau} + \sum_{k \neq 0} \frac{i \exp(ik\Omega\tau)}{k\Omega} \frac{\partial f_k}{\partial Y} f_{-k\tau}, \end{aligned} \tag{3.9}$$

for $t \geqslant \tau$. *For* Ω *sufficiently large, the averaged solution* X *exists in the interval* $[0, t_{max}]$. *Furthermore, for the approximation at stroboscopic times, we may write*

$$\max_{0 \leqslant t^{(k)} \leqslant t_{max}} \| x(t^{(k)}) - X(t^{(k)}) \| = \mathcal{O}\left(\frac{1}{\Omega^2}\right), \qquad \Omega \to \infty.$$

We point out that, for $t \geqslant \tau$, the dependence of $\dot{X}(t)$ on the past values $X(s)$, $-\tau \leqslant s < t$ is through *both* $Y(t) = X(t-\tau)$ *and* $Z(t) = X(t-2\tau)$; this is to be compared with the situation for the original oscillatory system (2.1), which does not include the delay 2τ. The functions $F^{(1)}$ and $F^{(2)}$ are of class C^2, but of course F is discontinuous at $t = \tau$. By implication, $X(t)$ will be of class C^3 except at $t = 0, \tau$ (where $\dot{X}(t)$ has a jump discontinuity), at $t = 2\tau$ (where the second derivative jumps) and $t = 3\tau$ (where the third derivative jumps).

In the particular case where f does not depend on the delayed argument y, so that we are dealing with an ordinary differential system, (3.8) and (3.9) are in agreement with formula (64) of Chartier et al. (2012).

4. Error analysis: exact micro-integration

In this section we investigate the global error of the algorithm under the assumption that the micro-integration is exact, so that the macro-integration and the numerical differentiations performed to find the slopes F_n are the only sources of error. This scenario is of course relevant when the micro-step h is chosen to be very small. The errors due to the Euler micro-integration will be studied in the next section.

In order to avoid misunderstandings, we state that 'exact micro-integration' has to be understood as follows. Consider e.g. the computation of $X_2, \ldots, X_N$ in Table 1; in this section we assume that

$$F_n = \frac{u_n(T) - u_n(-T)}{2T},$$

where u_n solves the problem $\dot{u}_n = f(u_n, v_n, \Omega t)$, $u_n(0) = X_n$, $v_n(t) = \varphi(-\tau + nH + t)$. Of course similar modifications of the algorithm in Table 1 have to be carried out for the computation of F_n for other values of n.

We begin by proving a stability bound for the macro-integrator. We consider a sequence $\{\hat{X}_n\}$ of vectors in $\mathbb{R}^D$ such that $\hat{X}_{-n} = \varphi(-nH)$, $n = 1, \ldots, N$, and furthermore satisfy the macro-integration equations with residuals $\{\hat{\rho}_n\}$, i.e.

$$\begin{aligned}
\hat{X}_1 &= \hat{X}_0 + HF^{(1)}(\hat{X}_0, \hat{X}_{-N}, 0; \Omega) + H\hat{\rho}_0, \\
\hat{X}_{n+1} &= \hat{X}_n + \frac{3H}{2}F^{(1)}(\hat{X}_n, \hat{X}_{n-N}, nH; \Omega) \\
&\qquad - \frac{H}{2}F^{(1)}(\hat{X}_{n-1}, \hat{X}_{n-1-N}, (n-1)H; \Omega) + H\hat{\rho}_n, \qquad n = 1, \ldots, N-1, \\
\hat{X}_{N+1} &= \hat{X}_N + HF^{(2)}(\hat{X}_N, \hat{X}_0, \hat{X}_{-N}; \Omega) + H\hat{\rho}_N, \\
\hat{X}_{n+1} &= \hat{X}_n + \frac{3H}{2}F^{(2)}(\hat{X}_n, \hat{X}_{n-N}, \hat{X}_{n-2N}; \Omega) \\
&\qquad - \frac{H}{2}F^{(2)}(\hat{X}_{n-1}, \hat{X}_{n-1-N}, \hat{X}_{n-1-2N}; \Omega) + H\hat{\rho}_n, \qquad n \geqslant N+1.
\end{aligned}$$

Furthermore we consider a second sequence $\{\tilde{X}_n\}$ with $\tilde{X}_{-n} = \varphi(-nH)$, $n = 1, \ldots, N$, satisying the macro-integration equations above with residuals $\{\tilde{\rho}_n\}$, rather than $\{\hat{\rho}_n\}$.

PROPOSITION 4.1 *To each bounded set $B \subset \mathbb{R}^D$, there corresponds a constant $C > 0$, independent of H and Ω, such that for any sequences $\{\hat{X}_n\}$ and $\{\tilde{X}_n\}$ as above contained in B,*

$$\|\hat{X}_n - \tilde{X}_n\| \leqslant C \sum_{k=0}^{n-1} H \|\hat{\rho}_k - \tilde{\rho}_k\|, \qquad 0 \leqslant nH \leqslant t_{max}.$$

Proof. From the hypotheses in the preceding section, F a Lipschitz continuous function of X, Y and Z with a Lipschitz constant that is uniform as t varies in the interval $0 \leqslant t \leqslant t_{max}$ and X, Y and Z vary in B. The stability bound is then proved in a standard way by recurrence. □

In our next result we investigate the consistency of the formulas (2.10)–(2.11) used to recover the slopes F_n. There are four cases corresponding to the four successive blocks in Table 1.

PROPOSITION 4.2 *The following results hold:*

1. *If the function u_n solves the problem*

$$\begin{aligned}
\dot{u}_n(t) &= f(u_n(t), \varphi(-\tau + t_n + t), \Omega t), \\
u_n(0) &= X_n,
\end{aligned}$$

then, with $Y_n = \varphi(-\tau + t_n)$,

$$\frac{u_n(T) - u_n(0)}{T} = f_0(X_n, Y_n) + \mathcal{O}(\frac{1}{\Omega}). \tag{4.1}$$

2. *If* u_n *is as in the preceding item, then*

$$\frac{u_n(T) - u_n(-T)}{2T} = f_0 + \sum_{k>0} \frac{i}{k\Omega} ([f_k - f_{-k}, f_0] + [f_{-k}, f_k]) - \sum_{k\neq 0} \frac{i}{k\Omega} \frac{\partial f_k}{\partial Y} \dot{\varphi}(-\tau + t_n) + \mathcal{O}(\frac{1}{\Omega^2}), \tag{4.2}$$

where f_k, $k \in \mathbb{Z}$ *are evaluated at* (X_n, Y_n), $Y_n = \varphi(-\tau + t_n)$.

3. *If u and v satisfy*

$$\begin{aligned} \dot{u}_n(t) &= f(u_n(t), v_n(t), \Omega t), \\ \dot{v}_n(t) &= f(v_n(t), w_n(t), \Omega t), \\ u_n(0) &= X_n, \\ v_n(0) &= Y_n, \\ w_n(0) &= Z_n, \end{aligned}$$

with w_n *a continuously differentiable function, then*

$$\frac{u_n(T) - u_n(0)}{T} = f_0(X_n, Y_n) + \mathcal{O}(\frac{1}{\Omega}). \tag{4.3}$$

4. *If u and v are as in 3., then*

$$\begin{aligned} \frac{u_n(T) - u_n(-T)}{2T} &= f_0 + \sum_{k>0} \frac{i}{k\Omega} ([f_k - f_{-k}, f_0] + [f_{-k}, f_k]) - \sum_{k\neq 0} \frac{i}{k\Omega} \frac{\partial f_k}{\partial Y} f_{0\tau} \\ &\quad + \sum_{k\neq 0} \frac{i}{k\Omega} \frac{\partial f_0}{\partial Y} f_{k\tau} + \sum_{k\neq 0} \frac{i}{k\Omega} \frac{\partial f_k}{\partial Y} f_{-k\tau} + \mathcal{O}(\frac{1}{\Omega^2}), \end{aligned} \tag{4.4}$$

where f_k, $k \in \mathbb{Z}$ *are evaluated at* (X_n, Y_n) *and* $f_{k\tau}$ *stands for* $f_k(Y_n, Z_n)$.

Proof. Here we prove the fourth case; the other proofs are similar (and slightly simpler). For simplicity the subindex n is dropped. We rewrite the equation for u as an integral equation

$$u(t) = X + \int_0^t f(u(s), v(s), \Omega s) ds.$$

and use Picard's iteration. Since, for $-T \leqslant t \leqslant T$,

$$u(t) = X + \mathcal{O}(\frac{1}{\Omega}),$$

we have

$$u(t) = X + t f_0(X, Y) + \sum_{k\neq 0} \alpha_k(t) f_k(X, Y) + \mathcal{O}(\frac{1}{\Omega^2}),$$

and, then,

$$\begin{aligned} u(t) &= X+\int_0^t \sum_{k\in\mathbb{Z}} \exp(ik\Omega s) \\ &\quad \times f_k\big(X+sf_0+\sum_{m\neq 0}\alpha_m(s)f_m+\mathscr{O}(\frac{1}{\Omega^2}),Y+sf_{0\tau}+\sum_{m\neq 0}\alpha_m(s)f_{m\tau}+\mathscr{O}(\frac{1}{\Omega^2})\big)ds. \end{aligned}$$

By Taylor expanding f at X,Y, we obtain, for $-T\leqslant t\leqslant T$:

$$\begin{aligned} u(t) &= X+tf_0+\sum_{k\neq 0}\alpha_k(t)f_k+\int_0^t s\frac{\partial f_0}{\partial X}f_0 ds+\int_0^t\sum_{k\neq 0}\alpha_k(s)\frac{\partial f_0}{\partial X}f_k ds \\ &\quad +\int_0^t\sum_{k\neq 0}\alpha_k(s)\frac{\partial f_0}{\partial Y}f_{k\tau}ds+\int_0^t s\frac{\partial f_0}{\partial Y}f_{0\tau}ds+\int_0^t\sum_{k\neq 0}\exp(ik\Omega s)s\frac{\partial f_k}{\partial X}f_0 ds \\ &\quad +\int_0^t\sum_{k,m\neq 0}\exp(ik\Omega s)\alpha_m(s)\frac{\partial f_k}{\partial X}f_m ds+\int_0^t\sum_{k\neq 0}\exp(ik\Omega s)s\frac{\partial f_k}{\partial Y}f_{0\tau}ds \\ &\quad +\int_0^t\sum_{k,m\neq 0}\exp(ik\Omega s)\alpha_m(s)\frac{\partial f_k}{\partial Y}f_{m\tau}ds+\mathscr{O}(\frac{1}{\Omega^3}). \end{aligned}$$

The proof concludes by evaluating this expression at $t=\pm T$ and taking those values to the left hand-side of (4.4). □

According to this result, (4.1) and (4.3) provide approximations with $\mathscr{O}(1/\Omega)$ errors to (3.8) and (3.9) (evaluated at $X=X_n, Y=X_n, t=t_n$) respectively, as expected from the use of forward differencing. Similarly (4.2) approximates (3.8) (at $X=X_n, Y=X_n, t=t_n$) with $\mathscr{O}(1/\Omega^2)$ error, as expected of central differences. However, when comparing (4.4) with (3.9) (at $X=X_n$, $Y=X_n$, $Z=Z_n$), we observe that the last sum in (3.9) has a factor $\exp(ik\Omega\tau)$, which is not present in the last sum in (4.4) and therefore the error is, in general, only $\mathscr{O}(1/\Omega)$. To achieve $\mathscr{O}(1/\Omega^2)$ errors we may assume that the functions $f_k(X,Y)$, $k\neq 0$, are independent of the second argument Y, i.e. the delay argument y only appears in f through f_0 (this is the case in (2.4)). Alternatively, we may assume that, for all $k\neq 0$, $\exp(ik\Omega\tau)=1$, i.e. that τ is an integer multiple of the period $T=2\pi/\Omega$.

We are now ready to give the main result of this section.

THEOREM 4.3 *Assume that the problem* (3.1)*, with the smoothness assumptions stated in the preceding section, is integrated with SAM with exact micro-integrations. In addition assume that one of the following hypotheses holds:*

- *(H1) The oscillatory Fourier coefficients f_k, $k\neq 0$ of f do not depend on the delayed argument y.*
- *(H2) The delay τ is an integer multiple of the period $T=2\pi/\Omega$.*

Then there exist constants Ω_0, H_0 and K such that, for $\Omega\geqslant\Omega_0$, $H\leqslant H_0$, $0\leqslant t_n=nH\leqslant t_{max}$, the difference between the numerical solution and the solution of the averaged problem has the bound

$$\|X_n-X(t_n)\|\leqslant K\left(H^2+\frac{H}{\Omega}+\frac{1}{\Omega^2}\right). \tag{4.5}$$

Proof. We apply Proposition 4.1 with B taken as a large ball containing the trajectory $X(t)$, $0\leqslant t\leqslant t_{max}$ in its interior; the vectors $X(t_n)$ play the role of $\tilde{X}_n$ and the vectors X_n play the role of $\hat{X}_n$. It is clear that

each $\tilde{X}_n$ is in B. For H sufficiently small and Ω sufficiently large the same will be true for each $\hat{X}_n$; this is established by means of a standard argument by contradiction using (4.5).

Each residual $\tilde{\rho}_n$ is $\mathscr{O}(H^2)$ with the exception of $\tilde{\rho}_0$, $\tilde{\rho}_N$ and $\tilde{\rho}_{2N}$; these are only $\mathscr{O}(H)$ because they first two correspond to Euler steps and in the third there is a jump discontinuity in the second time derivative of the averaged solution. According to Proposition 4.2, the residuals $\hat{\rho}_n$ for the numerical solution are $\mathscr{O}(1/\Omega^2)$, with the exception of $\hat{\rho}_0$ and $\hat{\rho}_N$, which are of size $\mathscr{O}(1/\Omega)$. Taking these results to Proposition 4.1, we get a global error bound of the desired form. □

Remark 1. It is clear that the bound in (4.5) may be replaced by one of the form $K'(H^2+1/\Omega^2)$. We prefer the form (4.5), as it relates to three sources of error: the macro-integration H^2 error, the error H/Ω arising from differencing at 0, τ, 2τ, and the error from second-order differencing at all other step points t_n.

Remark 2. The discrepancy between (4.4) and (3.9) that leads to the introduction of (H1) and (H2) stems from the fact that the values of the phase θ at t_n and $t_{n-N} = t_n - \tau$ are in general different in the oscillatory problem but the same in SAM. (H1) holds in most applications; (H2) is relevant in those studies where there is freedom in choosing the exact value of the large frequency Ω.

Remark 3. If (H1) and (H2) do not hold, the same proof yields a bound of the form $K(H^2+1/\Omega)$ under the assumption that f and φ are C^2 functions. Numerical experiments reveal that the bound cannot be improved to $K(H^2+1/\Omega^2)$. However in such a case it may be of interest to use an alternative, simpler algorithm based on applying forward differences at each step point t_n; obviously that alternative algorithm does not require the backward integration legs (2.9).

5. Error analysis: micro-integration errors

We now take into account the errors introduced by the Euler micro-integration. We begin with an auxiliary result. Note the improved error bound at the end of the integration interval.

PROPOSITION 5.1 *Consider the application of Euler's rule with constant step size $h = T/\nu_{max}$ to integrate in the interval $0 \leqslant t \leqslant T$ the initial value problem $\dot{u} = f(u, v, \Omega t)$, $u(0) = X$, where v is a known C^1 function. Denote by u_ν the Euler solution at $t = \nu h$. There are constants C, Ω_0 and h_0 such that for $h \leqslant h_0$, $\Omega \geqslant \Omega_0$, the following bounds hold:*

$$\|u_\nu - u(T)\| \leqslant Ch, \qquad \nu = 0, 1, \ldots, \nu_{max}. \tag{5.1}$$

$$\|u_{\nu_{max}} - u(T)\| \leqslant C\frac{h}{\Omega}, \tag{5.2}$$

$$\left\| \frac{u_{\nu_{max}} - X}{T} - \frac{u(T) - X}{T} \right\| \leqslant Ch. \tag{5.3}$$

Proof. A standard error bound for Euler's rule is

$$\|u_\nu - u(\nu h)\| \leqslant \frac{\exp(LT) - 1}{L} Mh, \qquad \nu = 0, \ldots, \nu_{max},$$

where L is the Lispchitz constant of f with respect to u in a neighbourhood of the solution and M is an upper bound for $\|(1/2)\ddot{u}(t)\|$, $0 \leqslant t \leqslant T$. In the present circumstances we have to take into account that, as $\Omega \to \infty$, the length $T = 2\pi/\Omega$ of the integration interval decreases and M grows like Ω, because

$$\ddot{u} = \frac{\partial f}{\partial u}\dot{u} + \frac{\partial f}{\partial v}\dot{v} + \Omega\frac{\partial f}{\partial t}.$$

From the elementary inequality $(\exp(LT)-1)/L \leqslant T\exp(LT)$ and the standard bound, we have

$$\|u_\nu - u(\nu h)\| \leqslant T\exp(LT)Mh, \qquad \nu = 0,\ldots,\nu_{max},$$

and therefore (5.1) holds.

By adding all the Euler equations we find

$$u_{\nu_{max}} = X + \sum_{\nu=0}^{\nu_{max}-1} hf(u_\nu, v(\nu h), \Omega\nu h),$$

and from (5.1),

$$u_{\nu_{max}} = X + \sum_{\nu=0}^{\nu_{max}-1} hf(u(\nu h), v(\nu h), \Omega\nu h) + \mathcal{O}(hT), \tag{5.4}$$

a relation that has to be compared with

$$u(T) = X + \int_0^T f(u(s), v(s), \Omega s)\, ds. \tag{5.5}$$

The bound (5.2) will be established if we show that the quadrature sum in (5.4) approximates the integral in (5.5) with errors of size $\mathcal{O}(hT)$. To this end we decompose the function being integrated as

$$f(u(s), v(s), \Omega s) = f(X, v(0), \Omega s) + \Big(f(u(s), v(s), \Omega s) - f(X, v(0), \Omega s)\Big) = f_1 + f_2.$$

It is easily seen (for instance by expanding in a Fourier series) that the total time derivative $(d/dt)f_2$ remains bounded as $\Omega \to \infty$; elementary results then show that the quadrature of f_2 has errors of the desired size $\mathcal{O}(hT)$. On the other hand, the time derivative of f_1 grows like Ω, and quadrature errors of size $\mathcal{O}(h)$ may be feared. Fortunately the quadrature for f_1 is actually exact, because one checks by an explicit computation that it is exact for each Fourier mode $f_k(X, v(0))\exp(ik\Omega s)$.

The third bound (5.3) is a trivial consiquence of (5.2). □

It goes without saying that the corresponding result holds for backward integrations with $-T \leqslant t \leqslant 0$. The following theorem provides the main result of this paper.

THEOREM 5.2 *Assume that the problem* (3.1)*, with the smoothness assumptions stated in the preceding sections, is integrated with SAM. In addition assume that one of the following hypotheses holds:*

- *(H1) The oscillatory Fourier coefficients f_k, $k \neq 0$ of f do not depend on the delayed argument y.*
- *(H2) The delay τ is an integer multiple of the period $T = 2\pi/\Omega$.*

Then there exist constants Ω_0, H_0 h_0 and K such that, for $\Omega \geqslant \Omega_0$, $H \leqslant H_0$, $h \leqslant h_0$, $0 \leqslant t_n = nH \leqslant t_{max}$, the difference between the numerical solution and the solution of the averaged problem may be bounded as follows

$$\|X_n - X(t_n)\| \leqslant K\left(H^2 + \frac{H}{\Omega} + \frac{1}{\Omega^2} + h\right).$$

In particular, if the grids are refined in such a way that h is taken proportional to H/Ω (i.e. ν_{max} is taken proportional to N), then the bound becomes

$$\|X_n - X(t_n)\| \leqslant K'\left(H^2 + \frac{H}{\Omega} + \frac{1}{\Omega^2}\right). \tag{5.6}$$

Proof. We argue as in Theorem 4.3. Now in the residual for the numerical solution $\{X_n\}$ we have to taken into account the micro-integration error. For $n \leqslant N$, the bound (5.3) (and the corresponding bound for the backward integration) show that the micro-integration adds a term of size $\mathscr{O}(h)$ to the residual. For $n > N$ the situation is slightly more complicated, because the algorithm uses past values $v_{n,v}$ that are themselves affected by micro-integration errors. However the stability of the micro-integrator guarantees that even when those errors are taken into account an estimate like (5.3) holds. □

We recall that taking h proportional to H/Ω makes the complexity of the algorithm independent of Ω.

6. Numerical experiments

We have integrated with SAM the toggle switch problem (2.4) with $\alpha = 2.5$, $\beta = 2$, $A = 0.1$, $\omega = 0.1$, $B = 4.0$, and $\tau = 0.5$. The function φ is constant: $x_1(t) = 0.5$, $x_2(t) = 2.0$, $-\tau \leqslant t \leqslant 0$, which corresponds to the system staying at an equilibrium up to time $t = 0$ and then switching on the slow and fast oscillatory forcing terms. For the macro-stepsize we set $H = \tau/N$, $N = 1,2,4,\ldots$ and the micro-stepsize was chosen as $h = T/(2N)$ (note that for the coarsest macro-step size $N = 1$, there are only two Euler steps per period).

Table 2 reports, for varying Ω and N, the maximum error, over $0 \leqslant t \leqslant 2$, in the X_1 component of the SAM solution with respect to the averaged solution obtained by integrating (2.5) (this integration was carried out with the Matlab function dde23 with relative and absolute tolerances 10^{-8} and 10^{-10} respectively). The combinations of N and Ω leading to values of H not significantly larger than T were not attempted, as the HMM idea does not make sense for them. Note that here τ/T is irrational and therefore the step points t_n are not stroboscopic times. Fig. 3 displays the errors in Table 2 as functions of N; for clarity not all values of Ω are included. By looking at the columns of the table (or at each of the four solid lines in the figure), we see that the error behaves as N^{-2}, i.e as H^2, except at the bottom of each column, where the behaviour is as N^{-1}. This is of course the behaviour of the bound in (5.6). Errors along rows saturate if Ω is very large; for those values one just observes the error in the macro-integration. This behaviour is also seen in the figure by comparing points corresponding to the same value of N and varying Ω. Along the main diagonal of the table, errors approximately divide by four, which is also in agreement with the bound (5.6). In the figure this corresponds to observing the behaviour of the right-most point of each of the solid lines.

Table 3 differs from Table 2 in that now Ω is taken from the sequence 8π, 16π, ... that consists of values not very different from those in Table 2. In fact the errors in Table 3 are very similar to those in Table 2. However for the sequence 8π, 16π, ... the step points are stroboscopic times and it makes sense to compare the SAM solution with the true oscillatory solution. The results are reported in Table 4. From Theorems 3.1 and 5.2 the errors with respect to the true solution possess a bound of the form (5.6) and this is consistent with the data in the table.

7. Extensions

We finally consider the application of SAM to problems that are not of the form (3.1). The number of variants that may arise is very high and we restrict the attention to reporting numerical results for a case study. (The corresponding analysis may be carried out by adapting the proofs given in the preceding sections.)

We study again the toggle switch problem, but now in an alternative asymptotic regime. The system

Table 2. Errors in x_1 for SAM with respect to the averaged solution for problem (2.4). Step points are not stroboscopic times

N	$\Omega = 25$	$\Omega = 50$	$\Omega = 100$	$\Omega = 200$	$\Omega = 400$	$\Omega = 800$	$\Omega = 1600$	$\Omega = 3200$
1	6.28(-2)	3.42(-2)	1.71(-2)	7.87(-3)	3.14(-3)	1.66(-3)	2.04(-3)	2.30(-3)
2	***	7.66(-3)	3.74(-3)	1.66(-3)	8.27(-4)	7.56(-4)	7.20(-4)	7.02(-4)
4	***	***	1.11(-3)	4.45(-4)	2.60(-4)	2.20(-4)	1.99(-4)	1.88(-4)
8	***	***	***	1.80(-4)	6.35(-5)	5.57(-5)	5.06(-5)	4.77(-5)
16	***	***	***	***	3.20(-5)	1.27(-5)	1.22(-5)	1.18(-5)
32	***	***	***	***	***	6.31(-6)	2.81(-6)	2.85(-6)
64	***	***	***	***	***	***	1.36(-6)	6.46(-7)
128	***	***	***	***	***	***	***	3.22(-7)

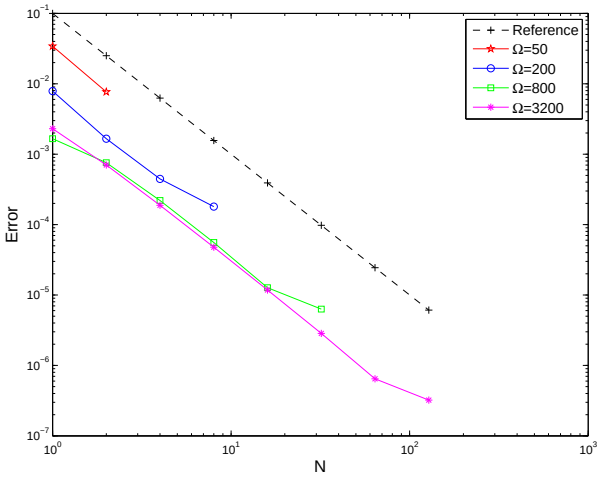

FIG. 3. Error in the first component of the SAM solution with respect to the solution of the averaged problem versus macro stepsize $H = \tau/N$ for some of the simulations in Table 2. Different lines correspond to difference values of Ω . Here the reference line shows the N^{-2} behaviour

Table 3. Errors in x_1 for SAM with respect to the averaged solution for problem (2.4). Step points are stroboscopic times

N	$\Omega = 8\pi$	$\Omega = 16\pi$	$\Omega = 32\pi$	$\Omega = 64\pi$	$\Omega = 128\pi$	$\Omega = 256\pi$	$\Omega = 512\pi$	$\Omega = 1024\pi$
1	6.25(-2)	3.40(-2)	1.70(-2)	7.82(-3)	3.11(-3)	1.66(-3)	2.04(-3)	2.30(-3)
2	***	7.62(-3)	3.72(-3)	1.65(-3)	8.26(-4)	7.56(-4)	7.20(-4)	7.02(-4)
4	***	***	1.11(-3)	4.42(-4)	2.59(-4)	2.20(-4)	1.99(-4)	1.88(-4)
8	***	***	***	1.78(-4)	6.34(-5)	5.57(-5)	5.06(-5)	4.77(-5)
16	***	***	***	***	3.16(-5)	1.26(-5)	1.22(-5)	1.18(-5)
32	***	***	***	***	***	6.24(-6)	2.80(-6)	2.85(-6)
64	***	***	***	***	***	***	1.35(-6)	6.47(-7)
128	***	***	***	***	***	***	***	3.18(-7)

Table 4. Errors in x_1 for SAM with respect to the true oscillatory solution for problem (2.4). Step points are stroboscopic times

N	$\Omega = 8\pi$	$\Omega = 16\pi$	$\Omega = 32\pi$	$\Omega = 64\pi$	$\Omega = 128\pi$	$\Omega = 256\pi$	$\Omega = 512\pi$	$\Omega = 1024\pi$
1	6.10(-2)	3.30(-2)	1.66(-2)	7.74(-3)	3.09(-3)	1.66(-3)	2.04(-3)	2.30(-3)
2	***	6.65(-3)	3.41(-3)	1.56(-3)	8.31(-4)	7.57(-4)	7.20(-4)	7.02(-4)
4	***	***	7.95(-4)	3.56(-4)	2.63(-4)	2.21(-4)	1.99(-4)	1.88(-4)
8	***	***	***	9.25(-5)	6.62(-5)	5.64(-5)	5.07(-5)	4.77(-5)
16	***	***	***	***	1.50(-5)	1.34(-5)	1.23(-5)	1.18(-5)
32	***	***	***	***	***	3.03(-6)	2.95(-6)	2.88(-6)
64	***	***	***	***	***	***	6.44(-7)	6.76(-7)
128	***	***	***	***	***	***	***	1.43(-7)

Table 5. Errors in x_1 for SAM with respect to the averaged solution for problem (7.1).

N	$\Omega = 8\pi$	$\Omega = 16\pi$	$\Omega = 32\pi$	$\Omega = 64\pi$	$\Omega = 128\pi$	$\Omega = 256\pi$	$\Omega = 512\pi$	$\Omega = 1024\pi$
1	4.10(-2)	4.09(-2)	4.08(-2)	4.08(-2)	4.08(-2)	4.07(-2)	4.07(-2)	4.07(-2)
2	***	8.08(-3)	7.89(-3)	7.81(-3)	7.77(-3)	7.76(-3)	7.75(-3)	7.75(-3)
4	***	***	1.78(-3)	1.70(-3)	1.67(-3)	1.65(-3)	1.64(-3)	1.64(-3)
8	***	***	***	4.29(-4)	4.08(-4)	3.99(-4)	3.99(-4)	4.06(-4)
16	***	***	***	***	1.06(-4)	1.01(-4)	1.04(-4)	1.07(-4)
32	***	***	***	***	***	2.62(-5)	2.50(-5)	2.68(-5)
64	***	***	***	***	***	***	6.53(-6)	6.47(-6)
128	***	***	***	***	***	***	***	1.63(-6)

is given by

$$\begin{aligned} \frac{dx_1}{dt} &= \frac{\alpha}{1+x_2^\beta} - x_1(t-\tau) + A\sin(\omega t) + \hat{B}\Omega\sin(\Omega t), \\ \frac{dx_2}{dt} &= \frac{\alpha}{1+x_1^\beta} - x_2(t-\tau), \end{aligned} \tag{7.1}$$

where $\hat{B}$ is a constant and the other symbols are as before. As $\Omega \to \infty$, the variable x_1 undergoes oscillations of frequency Ω and $\mathscr{O}(1)$ amplitude, which, for Ω large, makes the direct numerical integration of the system more expensive than that of (2.4) (the amplitude there is $\mathscr{O}(1/\Omega)$). For an analytic treatment, we begin by performing, for $t \geqslant 0$, the preliminary stroboscopic change of variables

$$\begin{aligned} x_1 &= X_1 + \hat{B}(1-\cos(\Omega t)), \\ x_2 &= X_2, \end{aligned}$$

which differs from the identity in $\mathscr{O}(1)$ quantities. This leads to:

$$\begin{aligned} \frac{dX_1}{dt} &= \frac{\alpha}{1+X_2^\beta} - X_1(t-\tau) - \hat{B}\,1_{\{t\geqslant\tau\}} + A\sin(\omega t), \\ \frac{dX_2}{dt} &= \frac{\alpha}{1+\left(X_1+\hat{B}(1-\cos(\Omega t))\right)^\beta} - X_2(t-\tau). \end{aligned} \tag{7.2}$$

The highly oscillatory forcing has been reduced from $\mathscr{O}(\Omega)$ to $\mathscr{O}(1)$ and, in principle, it is possible to average (7.2) by the techniques used to deal with (3.1). Unfortunately, finding the required Fourier coefficients in closed form does not appear to be possible in general. In the particular case where $\beta = 2$, the 0-Fourier coefficient may be found by evaluating the relevant integral (3.6) with the help of the residue theorem. This leads to the averaged system of the form $\dot{X} = f_0$ explicitly given by

$$\begin{aligned} \frac{dX_1}{dt} &= \frac{\alpha}{1+X_2^2} - X_1(t-\tau) - \hat{B}\,1_{\{t\geqslant\tau\}} + A\sin(\omega t), \\ \frac{dX_2}{dt} &= \alpha\frac{\sqrt{-\frac{M}{2}+\frac{\sqrt{N}}{2}} + (X_1+\hat{B})\sqrt{\frac{M}{2}+\frac{\sqrt{N}}{2}}}{\left(\frac{M}{2}+\frac{\sqrt{N}}{2}\right)^2 + (U+\hat{B})^2 + \sqrt{N}} - X_2(t-\tau), \end{aligned} \tag{7.3}$$

with $M = X_1^2 + 2\hat{B}X_1 - 1$, $N = M^2 + 4(X_1+\hat{B})^2$, whose solutions approximate x with errors of size at least $\mathscr{O}(1/\Omega)$ at stroboscopic times. However, since (7.2) is even in Ω, in this particular case the errors are actually $\mathscr{O}(1/\Omega^2)$.

Table 5 presents the errors in the SAM solution measured with respect to the solution of (7.3). The experiments have $\hat{B} = 0.1$; all other details are as in the preceding section. The table shows that the performance of SAM is very similar to that encountered in problem (2.4). We also measured errors with respect to the oscillatory solution and found that they are very close to those reported here, i.e. the situation is similar to that seen when comparing Tables 3 and 4.

Finally we mention that, for the choice of constants considered here, the integration (in the interval $0 \leqslant t \leqslant 2$) of the oscillatory problem for $\Omega = 1024\pi$ with dde23 in a laptop computer took more than 9,000 seconds. The corresponding SAM solution with the smallest value of H takes approximately one second. Since as pointed out before, the study of vibrational resonance requires integrations in time intervals two orders of magnitude larger than $0 \leqslant t \leqslant 2$, for many choices of the values of the constant that appear in the model, it is clear that a direct numerical integration of the oscillatory problem is not feasible for large values of Ω.

Acknowledgements. J.M. Sanz-Serna has been supported by projects MTM2013-46553-C3-1-P from Ministerio de Economía y Comercio, and MTM2016-77660-P(AEI/FEDER, UE) from Ministerio de Economía, Industria y Competitividad, Spain. Beibei Zhu has been supported by the National Natural Science Foundation of China (Grant No. 11371357). She is grateful to Universidad Carlos III de Madrid for hosting the stay in Spain that made this work possible and to the Chinese Scholarship Council for providing the necessary funds. The authors are thankful to M. A. F. Sanjuán and A. Daza for bringing to their attention the vibrational resonance phenomenon, the toggle switch problem and other highly-oscillatory systems with delay.

REFERENCES

ARIEL, G., ENGQUIST, B. & TSAI, R. (2009) A multiscale method for highly oscillatory ordinary differential equations with resonance. *Math. Comput.* **78**, 929-956.

CALVO, M. P., CHARTIER, PH., MURUA A. & SANZ-SERNA, J. M. (2011a) Numerical stroboscopic averaging for ODEs and DAEs. *Appl. Numer. Math.* **61**, 1077-1095.

CALVO, M. P., CHARTIER, PH., MURUA, A. & SANZ-SERNA, J. M. (2011b) A stroboscopic method for highly oscillatory problems. *Numerical Analysis and Multiscale Computations* (B. Engquist & O. Runborg & R. Tsai eds). New York: Springer, pp. 73-87.

CALVO, M. P. & SANZ-SERNA, J. M. (2009) Instabilities and inaccuracies in the integration of highly oscillatory problems. *SIAM J. Sci. Comput.* **31**, 1653-1677.

CALVO, M. P. & SANZ-SERNA, J. M. (2010) Heterogeneous Multiscale Methods for Mechanical Systems with Vibrations. *SIAM J. Sci. Comput.* **32**, 2029-2046.

CHARTIER, PH., MURUA, A. & SANZ-SERNA, J. M. (2010) Higher-order averaging, formal series and numerical integration I: B-series. *Found. Comput. Math.* **10**, 695-727.

CHARTIER, PH., MURUA, A. & SANZ-SERNA, J. M. (2012) Higher-order averaging, formal series and numerical integration II: the quasi-periodic case. *Found. Comput. Math.* **12**, 471-508.

CHARTIER, PH., MURUA, A. & SANZ-SERNA, J. M. (2015) Higher-order averaging, formal series and numerical integration III: error bounds. *Found. Comput. Math.* **15**, 591-612.

DAZA, A., WAGEMAKERS, A., RAJASEKAR, S. & SANJUÁN, M. A. F. (2013) Vibrational resonance in a time-delayed genetic toggle switch. *Commun. Nonlinear Sci. Numer. Simul.* **18**, 411-416.

E, W. (2003) Analysis of the heterogeneous multiscale method for ordinary differential equations. *Comm. Math. Sci.* **1**, 423-436.

E, W. & ENGQUIST, B. (2003) The heterogeneous multiscale methods. *Comm. Math. Sci.* **1**, 87-132.

E, W., ENGQUIST, B., LI, X., REN, W. & VANDEN-EIJNDEN, E. (2007) The hetergenous multiscale method: a review. *Commun. Comput. Phys.* **2**, 367-450.

ENGQUIST, B. & TSAI, Y. H. (2005) Hetergenous multiscale methods for stiff ordinary differential equations. *Math. Comput.* **74**, 1707-1742.

GARDNER, T. S., CANTOR, C. R. & COLLINS, J. J. (2000) Construction of a genetic toggle switch in Escherichia coli. *Nature*, **403**, 393-342.

HAIRER, E., LUBICH, CH. & WANNER, G.(2002) *Geometric Numerical Integration: Structure-Preserving Algorithms for Ordinary Differential Equations*. New York: Springer.

ISERLES, A. & NØRSETT, S. P.(2005) Efficient quadrature of highly oscillatory integrals using derivatives. *Proc. R. Soc. A.* **461**, 1383-1399.

LANDA, P. S. & MCCLINTOCK, P. V. E. (2000) Vibrational resonance. *J. Phys. A: Math. Gen.* **33**, L433.

LEHMAN, B. & WEIBEL, S. P.(1999) Fundamental theorems of averaging for functional differential equations. *J. Diff. Eqns.* **152**, 160-190.

LI, J., KEVREKIDIS, P. G., GEAR, C. W. & KEVREKIDIS, I. G. (2007) Deciding the nature of the coarse equation through microscopic simulations: the baby-bathwater scheme. *SIAM Rev.* **49**, 469-487.

SANZ-SERNA, J. M. (2009) Modulated Fourier expansions and heterogeneous multiscale methods. *IMA J. Numer. Anal.* **29**, 595-605.